

SEISMIC DELINEATION OF A GEOTHERMAL RESERVOIR IN THE MONTEVERDI AREA FROM VSP DATA

Gian Mauro Cameli¹, Fausto Batini¹, Ivano Dini¹, Jung Mo Lee², Richard L. Gibson¹
and M. Nafi Toksöz²

¹ENEL SpA/DPT/VDT-G, Via A. Pisano 120, 56122 Pisa, Italy

²Massachusetts Institute of Technology, 42 Carleton St., E34-462, Cambridge, MA

Keyword: Larderello geothermal field, vertical seismic profiling (VSP), inversion, migration

ABSTRACT

Surface seismic reflection surveys and VSP's have been extensively carried out in the Monteverdi area, within the Larderello region. Calibration of these seismic observations with data from numerous deep wells allowed the interpretation of the 2D traverses so that a good geologic-structural reconstruction for the whole area was achieved. Many important reflectors were detected inside the Metamorphic basement by VSP's acquired in several wells in the area. These reflections were attributed to changes in petrophysical characteristics of the medium, particularly changes in fracture density, rather than to contrasts in lithology.

Since at this time the main goal of the exploration in the Larderello region is the location of producing layers inside the basement, a major effort was applied to acquiring and modeling numerous VSP's in existing wells. In particular, a multioffset VSP was carried out in the COLLA 2 well with the specific goal of detecting fractured horizons within the reservoir of the Monteverdi area. Because of the three-dimensionality of the seismic wave propagation in such a complicated geological structure, the standard one-dimensional VSP modeling is not reliable. Therefore, 2D and 3D methods of modeling were applied.

The modeling of the VSP data predicts important reflections at the depths corresponding to the main fractured zones intersected by drilling. These fractured zones should show subhorizontal distribution and thickness of tens of meters

1. INTRODUCTION

The Larderello geothermal field located in central Italy, is a system of the hydrothermal type. Geothermal energy in this region has been exploited for almost a half century. Production from the shallow reservoirs (less than 1 km) has declined since the early 1970's, such that deep reservoirs are now the objective of geothermal exploration. Systematic geological and geophysical surveys such as gravity surveys (OGS, 1983), 2D and 3D surface reflection seismic surveys (Batini *et al.*, 1990; Batini *et al.*, 1991), and teleseismic traveltime inversion (Foley *et al.*, 1992) have established the regional structure of this area and have determined that the deep reservoirs are fractured zones within the Metamorphic basement, roughly 2-to-4-km-deep from the ground level.

The purpose of the present study is to delineate these deep reservoirs in the Monteverdi area using multi-offset VSP data from the Colla 2 well in conjunction with other geophysical and geological information. The goal will be achieved by means of (1) traveltime inversion to determine the velocity structure to the bottom of the VSP survey interval, (2) determining the up-going waves reflected from within and below the survey interval utilizing the previously obtained velocity structure and seismic data processing techniques, and (3) comparison of the observed VSP wavefields to numerical modeling of the wavefield

Table 1: Stratigraphy at the Colla 2 well

Depth (m)	Formation
0–50	Neogenic clayey and sandy formation
50–410	shale, marly limestone, and sandstone (Flysch formation)
410–630	Limestone
630–780	Anhydrite and dolomitic limestone
780–3754	Phyllite, mica schist, arid gneiss (Metamorphic basement)

2. COLLA 2 WELL

The Colla 2 well is a 4044-m production well located in the southern side of the Monteverdi area and about 2 km southeast of the Badia 1A production well. The well drifts northeastwardly reaching a vertical depth of 3754 m with total drift of about 1300 m (most drift occurs below 2000 m). The elevation of the well head is 220 m above sea level. The stratigraphy in the borehole is presented in Table 1. This stratigraphy shows strong correlation with the nearby Badia 1A well, and the formations appear to be subhorizontal.

The multi-offset three-component VSP experiment was carried out using two vertical vibrator sources. The VSP is the recording of seismic signals, generated by the seismic sources at the surface, by geophones at multiple depths in the well. The

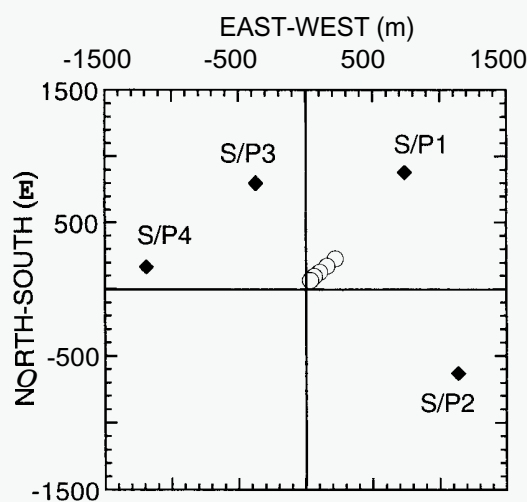


Figure 1: Locations of the four source offsets (the diamond symbols) used in the Colla 2 VSP experiment. The coordinates are relative to the well head. The well drift within the survey interval (1000 m ~ 3754 m) is presented by plotting the well locations every 250 m in depth.

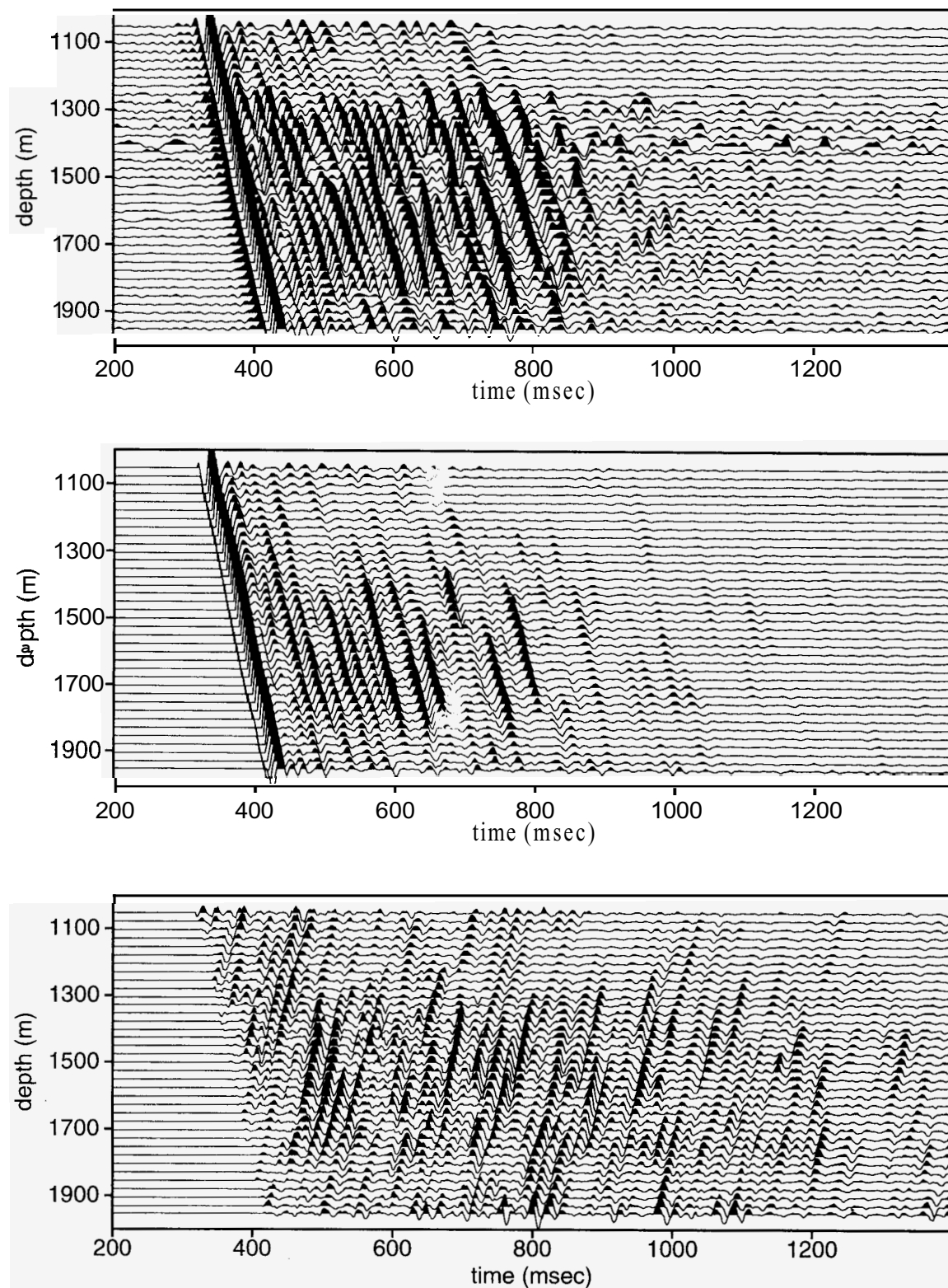


Figure 2: The vertical component of VSP data from S/P1: The original observed VSP section is presented at the top. The isolated down-going P-waves are presented in the middle. The isolated up-going P-waves are presented at the bottom. Note that the gain for the up-going P-wave plot is five times larger than the others.

source offsets are 1150 m at N40°E (S/P1), 1300 m at S61°E (S/P2), 880 m at N25°W (S/P3), and 1200 m at N82°W (S/P4) azimuth relative to the well head as shown in Figure 1. The source elevations relative to the well head are 160 m, -58 m, 50 m, and 77 m, respectively (negative being below the well head). Forty-one borehole receiver stations were distributed almost evenly in the depth interval of 1000 m to 2000 m. The differences in seismic arrival times as the receiver depth changes, are used to determine seismic velocity. This limited depth coverage provides only the average seismic velocity to a depth of 1000 m and interval velocities from depths of 1000 to 2000 m. The velocity structure is uncertain below 2000 m. As a result, the locations of reflectors below 2000 m are only estimated. However, by augmenting this velocity description with maps of the interfaces bounding the major geological units in the region and the VSP data from the nearby Badia 1A well (Gibson *et al.*, 1993), we can do three-dimensional modeling that accurately takes into account the most important seismic properties of the area.

3. DATA PROCESSING AND ANALYSIS

Wavefield separation: Raw VSP data have both down-going waves and reflected up-going waves. The up-going waves provide information on reflectors and their amplitude is smaller than those of down-going waves. Median filtering was used to extract up-going waves. Usually, the apparent velocity of an up-going wave is similar to that of the subtending down-going wave with a negative sign (identical in the zero-offset VSP case). Utilizing the first breaks (P arrival times), the down-going P-waves are aligned and extracted. The up-going P-waves are extracted using the negative velocity of the down-going P-waves. After the P-waves are removed, the down-going S arrival times are chosen and used to extract the up- and down-going S-waves. Figure 2 shows an example of wave separation from the vertical component of the total wavefield.

Traveltime Inversion: To estimate the velocity structure around the well within the surveyed interval, traveltime inversion is carried out using the first break times. Only 41 traveltimes are available for each source, and none of sources are on the same azimuth. As a result, the inversion problem is restricted to one dimension, that is velocity structure is assumed to vary with depth only. This restriction, however, still does not avoid the ill-posedness of the problem. A nonlinear inversion method combined with Tikhonov regularization is utilized to find the minimum structure solutions (see Lee *et al.*, 1992 for detailed algorithm).

Optimal results are obtained with the *trade-off parameter* (smoothness parameter) value of $10E6$, and are presented in Figure 3. Different static corrections for each source are necessary to get similar velocities within the top 1000 m depth interval. Inversion without static corrections provided unrealistic results. At shallow depths the seismic velocity structure varies significantly. The different velocities within depths of 1000 and 2000 m (the VSP survey interval) suggest strong horizontal inhomogeneity around the well. The velocity profile from the traveltime inversion was used as the background velocity for the migration imaging.

Kirchhoff Migration: Reflection seismic processing utilizes two important techniques to improve subsurface imaging. First, if the subsurface can be approximated by horizontal layers, the data from different source and receiver positions can be summed when they have the same subsurface reflection points. This is called stacking. Secondly, since the subsurface structure is not always flat layer, a significant portion of the seismic signal observed is in fact scattered rather than simply reflected. The

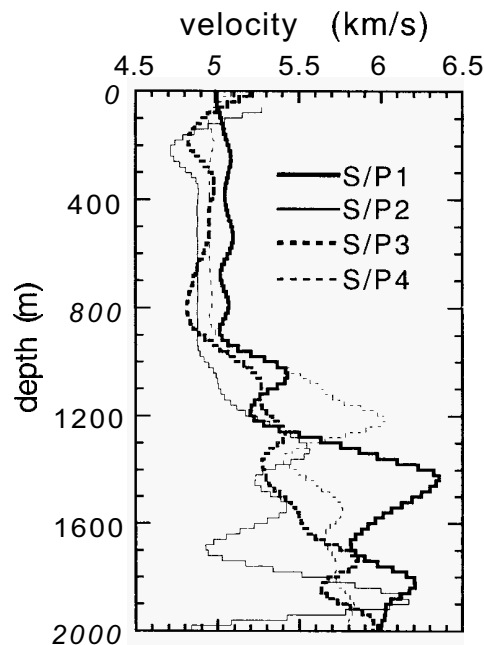


Figure 3: Optimal result of 1-D traveltime tomographic inversion: The Tikhonov regularization with the *trade-off parameter* value of $10E6$ was used to obtain the minimum structure solution. The thick solid line indicates S/P1, the thin solid line indicates S/P2, the thick dotted line indicates S/P3, and the thin dotted line indicates S/P4. Note the lateral inhomogeneity with the azimuths of shot points.

process by which these scattered signals are re-located to their place of origin is called migration. Both stacking and migration require description of the subsurface velocity structure in implementation.

The up-going P-waves were migrated, to delineate deep reflectors, using a 2.5-D common shot prestack inversion algorithm. The algorithm is a Kirchhoff-type inversion with laterally and depth-dependent propagation velocity. The 2.5-D feature provides out-of-plane spreading correction with prescribed background velocity structure (Dong *et al.*, 1991). Various background velocity models were defined from the results of the traveltime inversions. The best results are obtained using a velocity model of 8 layers with velocities of 3713, 5637, 5266, 5700, 5500, 5600, 5266, and 6000 m/s with corresponding interfaces at depths of 343, 763, 1003, 1303, 1503, 2003, and 3503 m. The migration images are presented in Figure 4.

Since the input VSP section data were band-limited (about two octaves), the smoothed images are also band-limited, which makes them appear somewhat sinusoidal. An apparent concave reflector intersects the well at a depth of 2000 m. This correlates in depth with a zone of weak permeability in phyllites and mica schists observed during production operation. However, the concave structure is uncertain because upward curvatures are typical artifacts in VSP migration (Payne *et al.*, 1994). Two strong and relatively flat reflectors at depths of about 3000 m and 4000 m are observed in all images. The slight variation of the depths of these reflectors for different source location suggests azimuthal velocity variation around the well.

4. RAY-BORN MODELING

The ray-Born algorithm uses the Born approximation to compute the amplitudes of wavefields scattered by small, localized heterogeneities superposed on a smoothly varying background earth model. Within the Born approximation, all propagation of elastic waves is controlled by the velocities and densities of

the background model (Gibson and Ben-Menahem, 1991; Wu and Aki, 1985). Ray tracing is used to compute the incident wavefield in this background medium and to propagate the scattered waves from the scattering heterogeneity back to the receiver (Fig. 5). In order for the ray tracing results to be accurate, the background model must be “smooth” in the sense that any heterogeneity involved must have a length scale much longer than a wavelength (Ben-Menahem and Beydoun, 1985).

The background earth model for the Colla 2 modeling task consists of 3 major layers, with the bounding interfaces obtained from other geophysical and geological studies — the base of the Flysch formation and the top of the Metamorphic basement. These interfaces are strongly nonplanar shapes which will lead to complicated ray paths from a given source position to a VSP

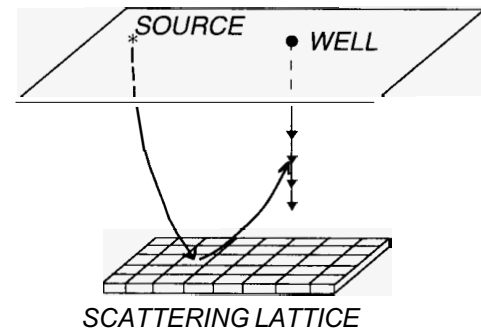


Figure 5: Schematic illustration of the ray-Born method: A scattering heterogeneous region within the earth is discretized into a lattice. Rays corresponding to the incident wavefield are traced from source to each elemental volume in the lattice, and rays are then traced from each point in the lattice to the receivers to compute the scattered wavefield. The Born approximation gives the amplitude of the scattered wave. A summation over all of the elemental volumes in the lattice (an integration) yields the total scattered field.

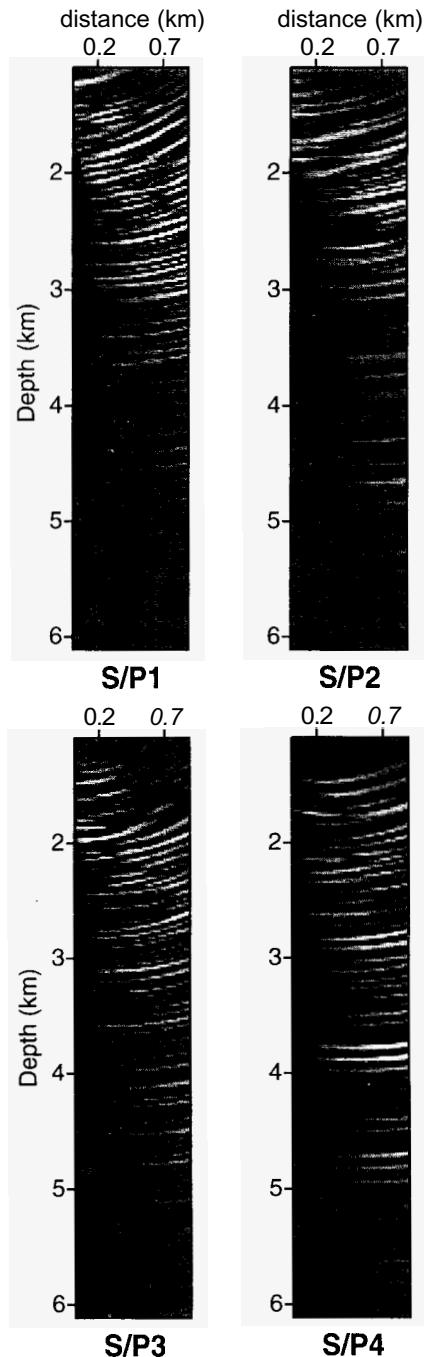


Figure 4: Kirchhoff migration image of four offsets with an 8-layer background velocity model: The well is located at the left of each image.

Table 2: Seismic parameters used in ray-Born modeling

Layer	Velocity (km/s)	Density (g/cc)
1	3.6	2.40
2	4.5	2.67
3	6.1	2.72

S-wave velocities were chosen by $V_s = V_p/\sqrt{3}$.

receiver (see Gibson *et al.*, 1994 for the detailed structure of the interfaces). Since the VSP section from S/P4 displayed some very strong reflections, we chose to begin analysis with data collected from this shot point. Initial estimates for the velocities of each layer were taken from inversion analysis of the down-going wavefield, and densities of the three layers were chosen to be the same as those used by Gibson *et al.* (1993). The velocity estimates were modified based on trial and error forward modeling until a good match to the observed arrival times was obtained. The P-wave velocity results are presented in Table 2.

Figure 6 shows that two major reflected P-wave events are apparent in the observed data after processing to extract up-going P-waves. The first arrives at about 790 ms at the bottom of the well and 950 ms at the most shallow receiver. The same times for the second event are 1100 ms and 1250 ms. In order to attempt to derive an estimate of the depth of the reflecting structures, we modeled the scattering from thin, planar structures such as potential producing fracture zones. For simplicity, the structures were constrained to be horizontal. The depths of the two scattering depths were adjusted based on a comparison of the arrival time of the computed scattered waves to the observed reflection arrival times until a relatively good match was obtained. The depths of the two scattering horizons that match the reflectors found in the migration images, are 2850 m and 3800 m relative to the well head.

In order to compute the ray-Born synthetic seismograms, several quantities were specified which control the amplitudes of the scattered waves. First, the thickness of the scattering regions were each set to 50 m. Second, the perturbations to P and S-wave velocity were each set to -10%. These quantities yield results comparable to the relative amplitudes seen in the data. The synthetic seismograms show that the match to the VSP data is reasonable, as shown in Figure 6. Synthetic seismograms included all of the effects of three-dimensional wave propagation.

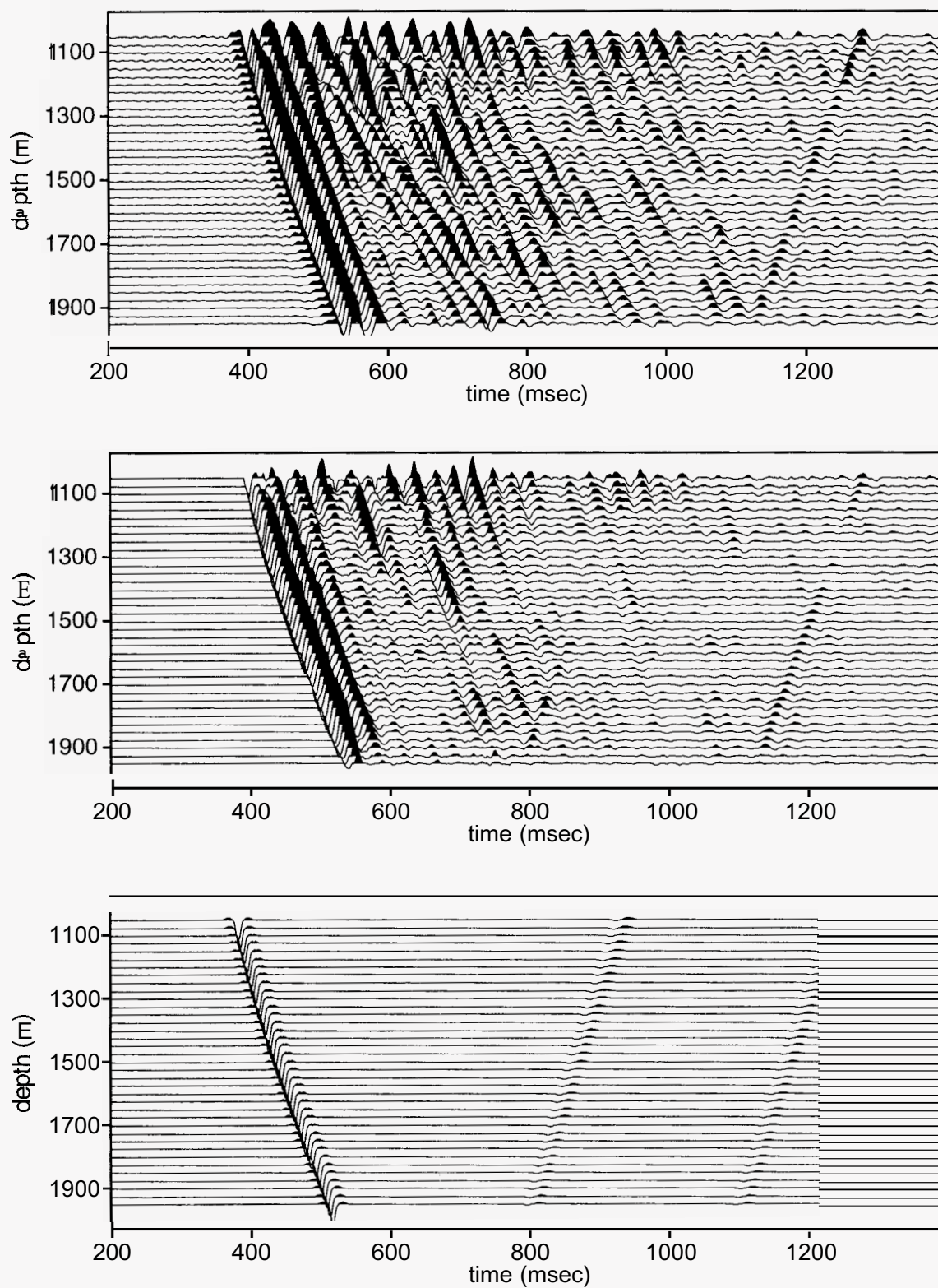


Figure 6: The vertical component of observed and synthetic VSP data from S/P4: The original observed VSP section is presented at the top. The isolated up- and down-going P-waves are presented in the middle. The synthetic up- and down-going P-waves are presented at the bottom. Note the good match in both time and amplitude.

This estimate supports the results of the migration imaging of the VSP data which was based more on traveltimes than on amplitudes.

The shallow reflector matches the fracture zone which presently produces eight tons of steam per hour (the major production zone in Colla 2 well). The deeper reflector matches the horizontally varying K horizon which is a major regional reflector (Batini *et al.*, 1983; Block, 1991).

Given the results obtained using the data from S/P4, an obvious first check on the results is to repeat the modeling using the data from another shot point. We attempted to do this using data from S/P2. The VSP section from S/P2 is of poor quality but it is interesting to observe that the down-going P-waves arrive significantly earlier in this data set than for S/P4. Model results with this data were much less satisfactory than S/P4. Using the same geometrical and velocity model as above, we failed to match the first breaks observed in the data. The error was actually quite large, and all synthetic travel times were about 100 ms too late. Hence, it is clear that our model does not account for all of the properties of the Colla 2 area.

Another possible explanation for the errors could be related to a problem with the geometric model. S/P2 had the lowest elevation of all the source points and was located at the bottom of a small river valley. The other sources appear to have been located above the valleys on hill slopes. For these reasons, it would not be too surprising if there were some local geological differences leading to different travel times. According to the model, the interface corresponding to the base of the Flysch formation should still be approximately 400 m below the shot point. We would not expect the seismic properties of this layer to be significantly different over a depth range of 400 m even given the unique location of S/P2. Yet the best fit to travel times of the model was obtained by setting the velocities in the first layer over this interface equal to the velocities of the second layer (Table 2), though the quality of the match was not as good as was found for S/P4. This would suggest that the higher velocity formation in the area below the S/P2 is found at a much shallower depth than is indicated by other geophysical and geological surveys. Even though the high velocity model did come close in matching traveltimes, it showed unusual amplitude errors which are probably related to some aspect of the shapes of the interfaces involved. Since a satisfactory model of the down-going waveforms was never obtained, we did not attempt to model scattered waves for S/P2.

5. CONCLUSIONS

We have analyzed the VSP data from the Colla 2 well in the Monteverdi area, in conjunction with other local geological and geophysical information. We have performed traveltime inversion to determine the velocity structure down to the base of the survey interval and Kirchhoff migration to image deep reflectors below the survey interval. The results of traveltime inversion showed strong lateral inhomogeneity, and provided the background velocity field for migration. One reflector at the bottom of the survey interval (2000 m) and two deep reflectors at depths of about 3000 m and 4000 m were interpreted from these migration images.

Modeling of these deep reflections was carried out using the S/P4 data. Application of a three-dimensional ray-Born modeling method yielded an accurate estimate of the locations of two reflecting features. Within the Metamorphic basement, the two structures were modeled as heterogeneous zones about 50 m thick, with velocity decreases of 10%. The modeling results confirmed the two deep reflectors found at depths of 2850 m and 3800 m. The more shallow reflector matches the presently producing fracture zone. The deeper reflector matches a commonly noted regional reflector, K horizon. We attempted to repeat the modeling for the data from S/P2, but were not able to accurately model the down-going waves using a model consistent with the model used to study the data from S/P4. This suggests some

errors in the background geological model, possibly related to the mapped depths of the base of the Flysch formation or to very large lateral changes in lithology with associated changes in seismic velocity.

This study has shown that, the seismic method in conjunction with geologic and other geophysical surveys can delineate geothermal reservoirs attributed to changes in petrophysical characteristics.

REFERENCES

- Batini, F., Bertini, G., Gianelli, Pandeli, E. and Puxeddu, **31**. (1983). Deep structure of the Larderello field: contribution from recent geophysical and geological data. *Mem. Soc. Geol. It.*, Vol.25, pp.219–235.
- Batini, F., Omnes, G. and Renoux, P. (1990). Delineation of geothermal reservoirs with **3-D** surface seismic and multi-offset WSPS in the Larderello area. *Geothermal Resource Council, Trans.*, Vol.14, pp. 1381–1386.
- Batini, F., Omnes, G. and Renoux, P. (1991). 3D surface seismic and well seismic applied to the delineation of geothermal reservoirs in metamorphic formations: in the Larderello area. *Abstr. European Assoc. Explor. Geophys. Annual Meeting*, pp.358–359.
- Ben-Menahem, A. and Beydoun, W. (1985). Range of validity of seismic ray and beam methods in general inhomogeneous media—I. General theory. *Geophys. J.R. astr. Soc.*, Vol.82(2), pp.207–234.
- Block, L. (1991). Joint hypocenter-velocity inversion of local earthquake arrival time data in two geothermal regions: Sc.D. thesis, Mass. Inst. Tech.
- Dong, W., Emanuel, M.J., Bording, P. and Bleistein, N. (1991). A computer implementation of 2.5-U common-shot inversion. *Geophys.*, Vol.56(9), pp.1384–1394.
- Foley J., Toksöz, M.N. and Batini, F. (1992). Inversion of teleseismic travel time residuals for velocity structure in the Larderello geothermal field, Italy. *Geophys. Res. Lett.*, Vol.19(1), pp.5–8.
- Gibson, R.L. and Ben-Menahem, A. (1991). Elastic wave scattering by anisotropic obstacles: application to fractured volumes. *J. Geophys. Res.*, Vol.96(B12), pp.19905–19924.
- Gibson, R.L., Lee, J.M., Toksöz, M.N., Dini, I. and Cameli, G.M. (1994). Three-dimensional Kirchhoff migration analysis of VSP data from a geothermal field. *In This Volume*.
- Gibson, R. L., Toksöz, M.N. and Batini, F. (1993). Ray-Born modeling of fracture zone reflections in the Larderello geothermal field. *Geophys. J. Int.*, Vol.114(1), pp.81–90.
- Lee, J.M., Matarese, J.M., Toksöz, M.N. and Turpening, W.R. (1992). Nonlinear traveltime tomography applied to M.I.T.'s Michigan test site. *Proc. 2nd SEGJ/SEG Int'l Symposium, Geotomography*, Vol.2, pp.457–471.
- O. G. S. (1984). Cnificazione dei rilievi gravimetrici nell'area geotermica toscana per l'ENEL Final Report, *Osservatorio Geofisico Sperimentale* report no.83597.
- Payne, M.A., Eriksen, E.A., and Rape, T.D. (1994). Considerations for high-resolution VSP imaging. *The Leading Edge*, Vol.13(3), pp.173–180.
- Wu, R.-S. and Aki, K. (1985). Scattering characteristics of elastic waves by an elastic heterogeneity. *Geophysics*, Vol.50(4), pp.582–595.